Materials Sciences and Applications, 2021, 12, 461-474
https://www.scirp.org/journal/msa
ISSN Online: 2153-1188
ISSN Print: 2153-117X

Influence of Annealing Atmosphere on Varistor Property of TiO_2-Nb_2O_5-$SrCO_3$ Ceramics

Kunyong Kang[1,2], Haodong Zhu[1,2], Gang Zhu[1,2*], Shuduan Deng[2*]

[1]Functional and Wood-Based Ceramics Laboratory, Southwest Forestry University, Kunming, China
[2]School of Materials Science and Engineering, Southwest Forestry University, Kunming, China
Email: *zhugangipm209@163.com, *1259932352@qq.com

How to cite this paper: Kang, K.Y., Zhu, H.D., Zhu, G. and Deng, S.D. (2021) Influence of Annealing Atmosphere on Varistor Property of TiO_2-Nb_2O_5-$SrCO_3$ Ceramics. *Materials Sciences and Applications*, **12**, 461-474.
https://doi.org/10.4236/msa.2021.1211030

Received: September 26, 2021
Accepted: November 7, 2021
Published: November 10, 2021

Abstract

Varistor ceramics are typical electronic ceramics, which are widely used in circuits of overvoltage protection, high voltage stabilization and high energy surge absorption. TiO_2 varistor ceramics has the advantages of low varistor voltage and good dielectric properties, but their low nonlinearity limited the application. The influence of annealing on the varistor properties of TiO_2-Nb_2O_5-$SrCO_3$ ceramics was investigated in this paper. TiO_2-Nb_2O_5-$SrCO_3$ varistor ceramics were prepared by the traditional method of ball grinding-forming-sintering and they were annealed in oxygen and nitrogen, respectively. The nonlinear coefficient α and the breakdown voltage E_B of the samples were tested using the varistor dc parameter meter. The microstructure of samples was analyzed by XRD, SEM, STEM-EDAX and SAEDP. The results show that during annealing, Sr^{2+} ions with a larger radius obtain the kinetic energy and are segregated to grain boundaries, which increases the acceptor density of the grain boundaries and improves α. Annealing in an oxygen atmosphere, the enrichment of oxygen at grain boundaries is also helpful to increase the density of acceptor states and the height of the potential barrier, so as to further increase α. Meanwhile, annealing makes crystalline grains grow properly, which results in even grain size, reduces the porosity and increases the density of grains. So E_B tends to reduce. As the doping concentration of Nb_2O_5 and $SrCO_3$ is 0.15 mol%, respectively, and sintering temperature is 1300˚C, TiO_2-Nb_2O_5-$SrCO_3$ varistor ceramics annealed in oxygen for 3 h at 750˚C achieved the highest nonlinear coefficient α = 8.9 and the lowest breakdown voltage E_B = 19.1 V·mm^{-1}, which annealed in nitrogen achieved α = 8.4, E_B = 20.6 V·mm^{-1}, both superior to unannealed samples.

Keywords

TiO_2, Nonlinear Coefficient, Breakdown Voltage, Annealing Atmosphere

1. Introduction

Varistor ceramics are typical electronic ceramics, which are widely used in circuits of overvoltage protection, high voltage stabilization and high energy surge absorption, because of their non-ohmic electrical properties and sensitivity to instantaneous voltage fluctuations [1]. For a given varistor, the non-ohmic properties depend on the structure of the grain boundary barrier of the polycrystalline ceramics [2]. Compared with ZnO and SnO_2 varistor ceramics, TiO_2 varistor ceramics has the advantages of low varistor voltage and good dielectric properties, which can be used as a varistor-capacitor multifunctional material. Furthermore, a simple preparation process makes it low cost. So it has a good application prospect [3]-[11]. Since the varistor properties of TiO_2 ceramics were discovered at Bell Labs in 1982 [2], the researchers have been tried to improve its nonlinearity, namely α value, by studying the effects of donor single-doping, acceptor single-doping and the co-doping of donor and acceptor on its varistor properties [12] [13] [14] [15]. Recently, S. Ekaphan *et al.* studied dielectric and nonlinear properties of $Ca_{1-1.5x}Pr_xCu_3Ti_4O_{12}/TiO_2$ ceramics. Nonlinear properties of the ceramics can be improved by doping with Pr^{3+} ions [16]. S. J. Yang *et al.* studied TiO_2-based varistor-capacitor ceramics co-doped with fixed Nb_2O_5, MnO_2, Sm_2O_3 and various contents of Sb_2O_3. The results indicate that the addition of Sb_2O_3 effectively decreases the breakdown voltage E_B (the voltage corresponding to the current J = 1 mA/cm^2), while having less impact on the nonlinear coefficient α [17]. F. C. Peng *et al.* studied TiO_2-based ceramics doped with various contents of Ho_2O_3 in the range of 0 - 0.6 mol%. The results show that the relative dielectric constant ε_r and the nonlinear coefficient α of samples firstly ascend and then descend with the increasing of Ho_2O_3 [18]. K.Y. Kang *et al.* investigated the influence of GeO_2 on α and E_B of TiO_2-Ta_2O_5-$CaCO_3$ varistor ceramics. The results show that GeO_2 doping changes the microstructures of TiO_2-Ta_2O_5-$CaCO_3$ ceramics, resulting in increased α and decreased E_B [19]. Although these methods of doping in the literature have a certain effect on improving the nonlinear coefficient α, it seems difficult to improve further α value by doping. So it is indispensable to seek new methods.

Annealing is a heat treatment that is used to adjust the microstructure and eliminate the defects of materials. Its technological process is heating the sample to a suitable temperature for a period of time, followed by slow cooling, so as to obtain a near equilibrium state of properties. R. Mannam *et al.* studied the reversible p-type properties of pulsed laser deposited (P, N) co-doped ZnO thin films. As the film grows, it changes from p-type to n-type over a period of 120 days. Non-annealed N-type films contained donor impurities hydrogen and carbon, and the films were transformed into p-type semiconductors after annealing at 800˚C [20]. D.M. Priyadarshini *et al.* studied the effect of the annealing environment on SnO_2 thin film transistors. The results showed that with the increase of nitrogen concentration, the performance of the equipment improves [21]. M.J. Zheng *et al.* studied the effect of annealing on GaN-based semicon-

ductor capacitors with ZrO_2 as dielectric layer prepared by atomic deposition method. The results showed that the capacitance gradually increased with the increase of annealing temperature from 300˚C to 500˚C [22]. A. Hosokawa *et al.* studied the effect of annealing on the properties of nano-composite Nd-Fe-Ti-B magnets. The results showed that A short time of annealing at a temperature close to the crystallization temperature can improve the magnetic properties, while a higher temperature and longer time of annealing would lead to the deterioration of magnetic properties [23]. J.Z. Zhao *et al.* studied the influence of annealing atmospheres on the varistor properties of TiO_2 varistors doped with Nb_2O_5 and Bi_2O_3. The results indicated that the height and width of the potential barrier and the breakdown voltage decrease when annealing in vacuum and H_2 [24]. It can be seen from these studies that annealing is effective in changing microstructures and improving some physical properties of materials.

In order to improve the nonlinear coefficient α of TiO_2 varistor ceramics and further reduce the breakdown voltage E_B, TiO_2-Nb_2O_5-$SrCO_3$ varistor ceramics are prepared by the traditional ceramics preparation process and annealed in different atmospheres in this work. The influence of annealing on the microstructure and the varistor properties of TiO_2-Nb_2O_5-$SrCO_3$ ceramics was studied.

2. Material and Methods

Table 1 shows the initial doping contents of each sample. The mixture was grinded in a planetary ball mill to obtain the reactants. The purity of each reagent is as follows: TiO_2 (powder, 99.9%), Nb_2O_5 (powder, 99.9%), $SrCO_3$ (powder, 99.9%). All reagents were obtained from Guanghua Sci-tech Co., Ltd, China. The mixture was grinded for 10 h according to the mass ratio of 1:2:4 of powder to water blended with alcohol (water: alcohol = 3:1) to balls. After homogenization, each blend was dried at 90˚C for 10 h and de-agglomerated in a 400 mesh sieve. The obtained powder was isostatically pressed at 160 MPa into tablets (10 mm in diameter and 1 mm thick). The tablets were degummed at 500˚C for 1 h in a box-type resistance furnace and sintered at 1250˚C, 1300˚C, 1350˚C, and 1400˚C for 3 h in a tube furnace, respectively. The tablets were cooled to room temperature through furnace cooling. The TiO_2-Nb_2O_5-$SrCO_3$ ceramic sheets obtained by the above method were coated with silver electrode. The varistor properties of all sheets were tested. Next, the samples with the best varistor properties

Table 1. Doping contents of samples.

Sample	Doping content/mol%		
	TiO_2	Nb_2O_5	$SrCO_3$
#1	99.80	0.10	0.10
#2	99.70	0.15	0.15
#3	99.60	0.20	0.20
#4	99.50	0.25	0.25

were annealed in oxygen and in nitrogen for 3 h at 650˚C, 700˚C, 750˚C and 800˚C, respectively, and the varistor properties of them were tested again. XRD was used to analyze the phase of samples. SEM was used to observe the morphology of the samples. STEM-EDAX was used to analyze the contents of each element in grains and at grain boundaries. SAEDP was used to analyze the crystallization degree of the samples.

3. Results and Discussion

3.1. Varistor Properties

Table 2 shows the values of the nonlinear coefficient α and the breakdown voltage E_B of samples with different doping concentrations sintered for 3 h at different temperatures. As can be seen from Table 2, when the sintering temperature is 1300˚C, TiO_2-Nb_2O_5-$SrCO_3$ varistor ceramics have better varistor properties (α = 6.2, E_B = 23.6 V·mm^{-1} for sample #2). Subsequently, the varistor properties of sample #2 sintered at 1300˚C were studied after annealing in oxygen and in nitrogen for 2, 2.5, 3, 3.5, and 4 h at 650˚C, 700˚C, 750˚C and 800˚C, respectively. Table 3 shows the electrical properties of the samples, where #O2 and #N2 represent the sample annealed in oxygen for 2 h or in nitrogen for 2 h,

Table 2. Electrical properties of samples with different sinter temperatures (E_B/V·mm^{-1}).

Sample	1250˚C		1300˚C		1350˚C		1400˚C	
	α	E_B	α	E_B	α	E_B	α	E_B
#1	2.5	27.2	5.4	24.1	4.2	26.8	4.8	25.3
#2	3.7	26.5	6.2	23.6	5.6	25.6	4.6	25.0
#3	3.4	28.3	5.6	23.3	5.2	27.5	4.7	22.6
#4	3.5	27.4	5.1	24.8	4.9	26.8	5.0	23.4

Table 3. Electrical properties of samples annealed for 2 - 4 h in air and in nitrogen (E_B/V·mm^{-1}).

Sample	time	650˚C		700˚C		750˚C		800˚C	
		α	E_B	α	E_B	α	E_B	α	E_B
#O2	2 h	6.8	24.7	7.0	21.3	7.3	23.5	7.0	23.3
#N2	2 h	6.5	23.1	6.5	23.2	7.5	23.2	7.1	21.6
#O2.5	2.5 h	6.5	22.4	7.3	22.6	8.1	22.7	7.5	20.5
#N2.5	2.5 h	6.9	21.3	7.2	21.5	8.0	23.0	7.5	19.8
#O3	3 h	7.1	23.2	7.7	23.5	8.9	19.1	8.0	23.1
#N3	3 h	6.8	22.7	7.5	23.3	8.4	20.6	7.9	21.7
#O3.5	3.5 h	7.2	21.7	7.7	21.8	7.9	21.2	7.2	21.3
#N3.5	3.5 h	7.1	22.0	7.4	20.2	7.8	22.4	7.4	23.4
#O4	4 h	6.7	23.3	7.0	22.5	7.4	22.0	7.2	22.8
#N4	4 h	6.8	21.8	7.3	22.8	7.2	22.4	6.9	21.9

respectively; #O3 and #N3 represent the sample annealed in oxygen for 3 h or in nitrogen for 3 h; #O2.5, #N2.5, #O3.5, #N3.5, #O4, and #N4, in a similar fashion. As can be seen from Table 3, the samples annealed at the same time at the same temperature in oxygen or in nitrogen show a slight difference in nonlinear coefficient α and breakdown voltage E_B. The sample annealed for 3 h at 750˚C in oxygen has the best varistor performance with $\alpha = 8.9$ and $E_B = 19.1$ V·mm^{-1}, the sample annealed for 3 h at 750˚C in nitrogen has the comparative performance with $\alpha = 8.4$ and $E_B = 20.6$ V·mm^{-1}, both superior to the unannealed sample with $\alpha = 6.2$ and $E_B = 23.6$ V·mm^{-1}. Annealing significantly improves the varistor performance of TiO_2-Nb_2O_5-$SrCO_3$ ceramics. With the increase of annealing temperature and annealing time, α value starts to decrease, which indicates that the annealing temperature and annealing time have a significant influence on the varistor performance of the samples.

Figure 1 is the I - V graph of the samples annealed in oxygen and in nitrogen for 3 h, where #O65 represents the sample annealed in oxygen at 650˚C for 3 h, and #N65 represents the sample annealed in nitrogen at 650˚C for 3 h; #O70 represents the sample annealed in oxygen at 700˚C for 3 h, and #N70 represents the sample annealed in nitrogen at 700˚C for 3 h; #O75, #N75, #O80, and #N80, in a similar fashion. The two samples annealed in oxygen and in nitrogen at the same temperature for 3 h show a slight difference in I - V graphs. However, the I - V graphs of the samples annealed at different temperatures show noteworthy differences. At the same annealing temperature, the I - V graph of the sample annealed in oxygen lies below that of the sample annealed in nitrogen, indicating the nonlinearity of the sample annealed in oxygen is slightly better than the sample annealed in nitrogen. The slopes of I - V graphs of the two samples annealed at 750˚C for 3 h in oxygen and in nitrogen are the minimum, indicating that α values are the maximum and the varistor properties are the best in all annealed samples. The average barrier height Φ_B at grain boundaries of sample #2, #O75 is calculated in light of the formula [25]

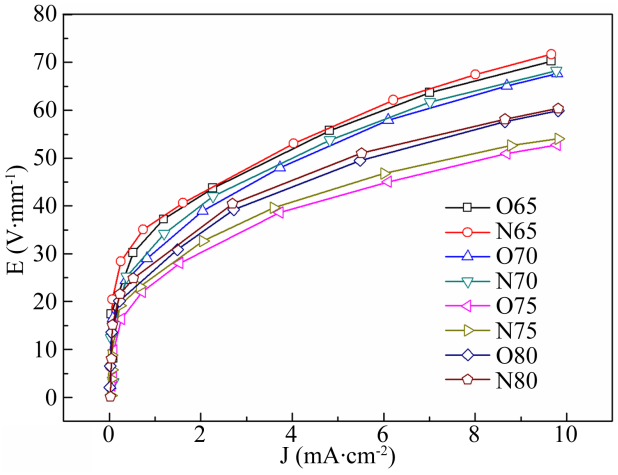

Figure 1. The I - V characteristics of TiO_2-Nb_2O_5-$SrCO_3$ ceramics annealed for 3 h at 650, 700, 750 and 800˚C in oxygen and nitrogen, respectively.

$$J = A^* T^2 \exp\left[\left(\beta E^{1/2} - \Phi_B\right)/kT\right] \quad (1)$$

where A^* and k represent the Richardson constant and the Boltzmann constant, respectively. T is the absolute temperature. The two groups of electric current J and electric field E were tested at the same temperature T. The values of β and Φ_B were calculated. Five Φ_B values were gotten for each sample and the average was listed in Table 4. From Table 4, the average potential barrier height Φ_B in #O75 and #N75 is higher than #2. Φ_B of #O75 is higher than #N75.

3.2. Microstructure Analysis

Figure 2 shows the XRD spectra of sample #2 (a), #O75 (b) and #N75 (c). It can be seen from Figure 2 that the backgrounds of diffraction peaks of the annealed

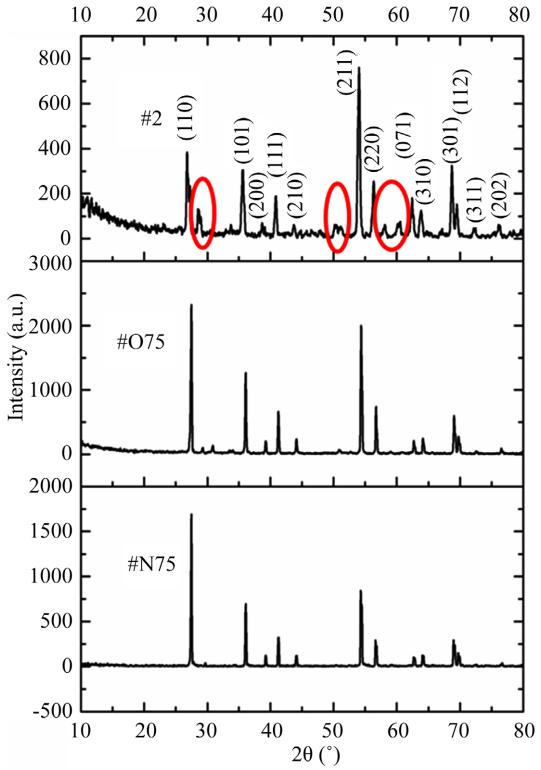

Figure 2. XRD patterns of TiO_2-Nb_2O_5-$SrCO_3$ ceramics unannealed (#2), annealed at 750˚C for 3 h in oxygen (#O75)and in nitrogen (#N75).

Table 4. Diffraction peak change near $2\theta = 27.5^\circ$ and average grain boundary barrier height of sample unannealed (#2), annealed at 750˚C for 3 h in air (#OA) and annealed at 750˚C for 3 h in nitrogen (#NA).

Sample	2θ (˚)	Peak Height	FWHM (˚)	Φ_B (eV)
#2	26.73	380.29	0.534	0.61
#O75	27.46	2304.36	0.334	0.73
#N75	27.46	1701.58	0.201	0.68

samples in oxygen (#O75) and nitrogen (#N75) are smoother than that of the unannealed sample (#2). And the intensity of diffraction peaks is increased, indicating that the grain growth of annealed samples is more complete. Before annealing, the additional diffraction peaks appear at 28.92˚, between 50˚ - 53˚ and between 57˚ - 62˚. After annealing, these diffraction peaks significantly weaken or disappear, indicating that a part of doping atoms with a smaller radius enter into TiO_2 lattice during annealing.

Table 4 shows the correlation parameters of the diffraction peaks near 2θ = 27˚ for sample #2, #O75 and #N75. The diffraction peak strength increases and the full width at half maximum (FWHM) decreases in sample #O75 and #N75, indicating the grains well-developed. The positions of the strongest diffraction peaks in the three samples are different. The strongest diffraction peak of the unannealed sample #2 is located at 2θ = 54.31˚, while that of the two annealed samples #O75 and #N75 are located at 2θ = 27.46˚. The diffraction peaks of #O75 and #N75 move to a higher angle, and the diffraction peak of #2 at 2θ = 28.92˚ disappears after annealing, indicating that the annealing causes atomics relaxation and ultimately improves the crystallization degree of the annealed samples.

Figure 3 shows SEM photographs of the fracture surface of sample #2 (a), #O75 (b), and #N75 (c). Comparing (a), (b) and (c), it can be seen that the grains of sample #O75 and #N75 are bigger with more uniform size and lower porosity than sample #2, which is conducive to good electrical properties. The grain boundary of #2 is more fuzzy than that of #O75 and #N75, which suggests the grains of #O75 and #N75 obtained second development during annealing.

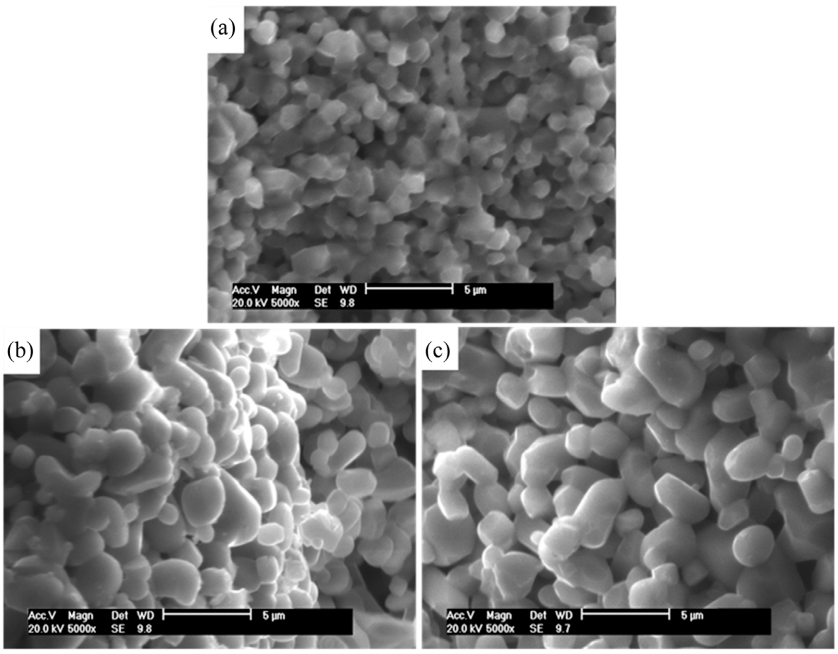

Figure 3. SEM images of TiO_2-Nb_2O_5-$SrCO_3$ ceramics unannealed (#2) (a), annealed at 750˚C for 3 h in oxygen (#O75) (b) and in nitrogen (#N75) (c).

Figure 4 is STEM images of sample #2 (a), #O75 (b) and #N75 (c). Points 1 and 2 are located in grains, and points 3 and 4 are located at grain boundaries in the three figures. The contents of elements at each point are recorded in Table 5. By analyzing element contents of adopted points, the content of element Sr at grain boundaries is higher in the annealed samples #O75 and #N75 than the unannealed sample #2. The reason is that Sr^{2+} ions with a larger radius

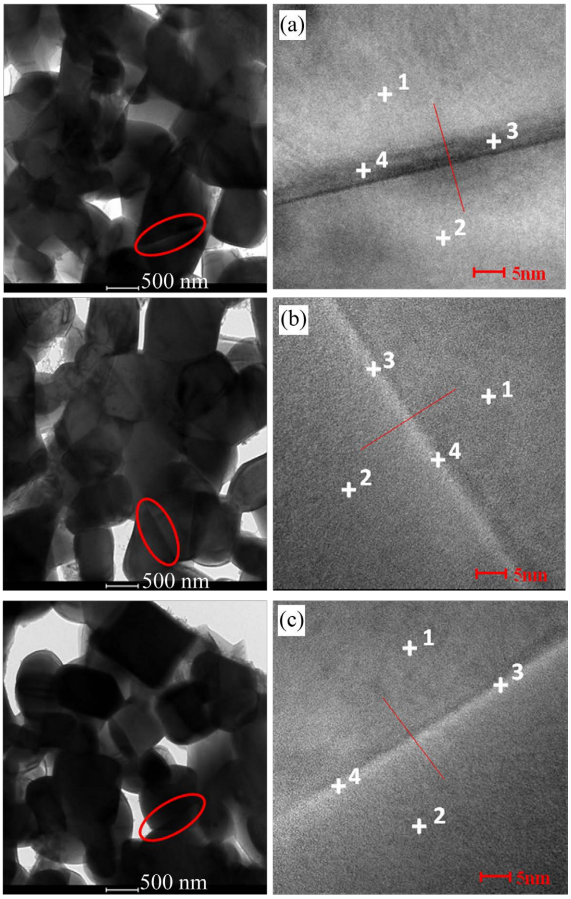

Figure 4. STEM-EDAX images of TiO_2-Nb_2O_5-$SrCO_3$ ceramics unannealed (#2) (a), annealed at 750˚C for 3 h in oxygen (#O75) (b) and in nitrogen (#N75) (c)

Table 5. Element contents in grains and at grain boundaries of sample unannealed (#2), annealed at 750˚C for 3 h in air (#O75) and annealed at 750˚C for 3 h in nitrogen (#N75).

Position	Element (At%)											
	OK			TiK			NbK			SrK		
	#2	#O75	#N75	#2	#O75	#N75	#2	#O75	#N75	#2	#O75	#N75
1	70.71	70.56	71.15	28.98	29.06	28.54	0.23	0.32	0.28	0.08	0.06	0.03
2	73.55	72.60	66.94	26.04	27.23	32.62	0.31	0.15	0.39	0.10	0.02	0.05
3	71.32	74.83	66.87	27.92	24.19	32.27	0.19	0.25	0.18	0.57	0.73	0.68
4	75.44	76.38	69.23	23.52	22.53	29.83	0.42	0.17	0.05	0.62	0.92	0. 89

obtains kinetic energy and then are segregated to grain boundaries in the annealing process. So the content of Sr^{2+} in the grains of the annealed samples in oxygen or nitrogen tends to decrease, while the content of Sr^{2+} at boundaries tends to increase. The content of element O of sample #O75 annealed in oxygen is higher than sample #2 and #N75 at grain boundary.

Figure 5 is the STEM-EDAX line scanning graph across the grain boundary of sample #2, #O75 and #N75. As shown in Figure 5(a), the oxygen concentration at the grain boundary of #O75 is higher. The reason for it is that the oxygen is enriched at the grain boundary for sample #O75 annealed in oxygen atmosphere [24], which is why the nonlinear coefficient of #O75 is slightly higher than that of #N75. In Figure 5(c), it can be seen that the element Sr tends to segregation towards grain boundary. After annealing, Sr content at grain boundary is much higher than that in grain. By the mutation of the Sr concentration at the grain boundary, the width of the grain boundary of the two annealed samples is estimated to be about 3.56 nm. In Figure 5(b) and Figure 5(d), elements Ti and Nb are randomly distributed in grains and grain boundaries.

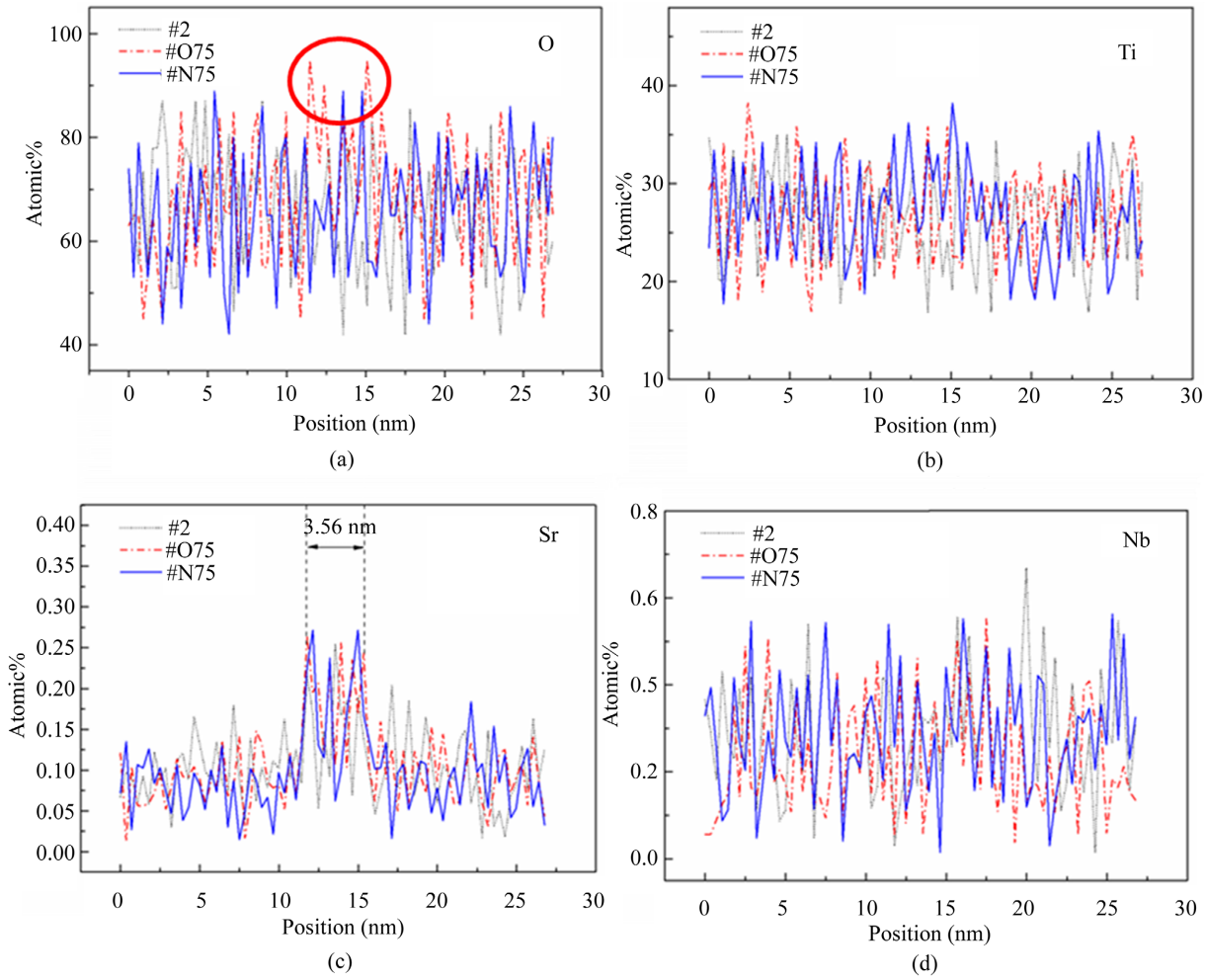

Figure 5. STEM-EDAX line scanning graph across grain boundary (shown in Figure 4) for sample #2 (unannealed), sample #O75 (annealed at 750˚C for 3 h in oxygen) and #N75 (annealed at 750˚C for 3 h in nitrogen).

Figure 6(a) and Figure 6(b) are the selected area electron diffraction patterns (SAEDP) of the grains in sample #2 and #O75, respectively. The electron diffraction pattern of unannealed sample #2 has the amorphous central diffraction spot and the polycrystalline diffraction rings. In the electron diffraction pattern of annealed sample #O75, the regular diffraction spot of single crystal is found, which indicated that the grains of annealed sample #O75 developed well.

3.3. Mechanism Analysis

A high α value and a low E_B value are required for TiO_2-based low voltage varistor. The barrier structure of grain boundary decides α and E_B. Increasing Φ_B can reduce the background current and decreasing X_D can improve the electron tunneling effect. Therefore, increasing Φ_B and decreasing X_D can improve α value. Φ_B is determined by the formula [26]

$$\Phi_B = e^2 N_S^2 / 2\varepsilon_0 \varepsilon_r N_D \tag{2}$$

where ε_0 is the dielectric constant of vacuum, ε_r is the relative dielectric constant of semi-conducting ceramic, N_D is the donor concentration in the semi-conductor depletion layer, N_S is the acceptor interface state density, e is electron charge. Decreasing N_D can increase Φ_B, and therefore increase α. But on the basis of the formula [27]

$$X_D = \sqrt{2\varepsilon_0 \varepsilon_r \Phi_B / eN_D} \tag{3}$$

decreasing N_D makes X_D increase and is not conducive to improving α. What is more, decreasing N_D reduces semi-conducting degree of grains, which goes against the low E_B. Therefore, the doping content of the donor has an optimal

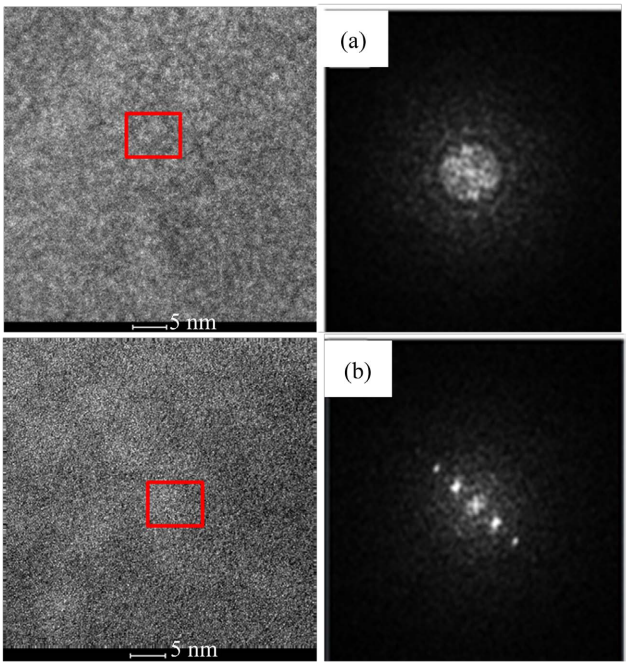

Figure 6. The contrast of the selected area electron diffraction patterns (SAEDP) for sample #2 (a), #O75 (b).

value. In like manner, increasing N_S makes Φ_B increase, and therefore increases α, but also increases X_D. Therefore, the doping content of the acceptor also has an optimal value. As the optimal doping content of the donor and the acceptor is determined, adjusting the doping content of the donor and the acceptor can't optimize α and E_B any longer, but appropriate annealing can further optimize α and E_B of the TiO_2-Nb_2O_5-$SrCO_3$ varistor ceramic. This can be explained as follows. The nonlinear coefficient of TiO_2-Nb_2O_5-$SrCO_3$ varistor ceramics can be appropriately improved by annealing, mainly because Sr^{2+} is segregated towards the grain boundary as far as possible in the annealing process, which increases the density of acceptor state and the height of potential barrier at grain boundaries. Annealing in the oxygen atmosphere, the oxygen enrichment at grain boundaries is also helpful to increase the density of acceptor states and the height of potential barrier, so as to further improve the nonlinear coefficient. Annealing at appropriate temperature for appropriate time can make the grains grow appropriately; the grain size even and the porosity reduce. Meanwhile, the number of grain boundaries and the total area of grain boundaries decrease. Therefore the breakdown voltage E_B tends to decrease.

4. Conclusion

In this work, it is found that annealing can further improve the microstructure of TiO_2-Nb_2O_5-$SrCO_3$ varistor ceramics and enhance the nonlinear coefficient α. During annealing, the acceptor ions Sr^{2+} with larger radius are further segregated towards the grain boundaries because of obtaining kinetic energy, which increases the density of acceptor state and the height of potential barrier at grain boundaries. Therefore α increases. Annealing in an oxygen atmosphere, the enrichment of oxygen at grain boundaries is also helpful to increase the density of acceptor states and the height of the potential barrier, so as to further increase the nonlinear coefficient. Annealing at the appropriate temperature for an appropriate time can make the grains grow appropriately, the grain size even and the porosity reduce, which results in the number of grain boundaries and the total area of grain boundaries decreasing. Therefore the breakdown voltage E_B tends to decrease. As the doping concentration of Nb_2O_5 and $SrCO_3$ is 0.15 mol%, respectively, and the sintering temperature is 1300˚C, TiO_2-Nb_2O_5-$SrCO_3$ varistor ceramics are annealed for 3 h at 750˚C in oxygen possess best varistor performance with α = 8.9 and E_B = 19.1 V·mm^{-1}. With further selecting dopants and optimizing annealing temperature, TiO_2 varistor ceramics are expected to obtain higher nonlinear coefficients and realize their practical application.

Acknowledgements

The present work was supported by the Agricultural Joint Programs of Yunnan Province [grant number 2018FG001-063], the University-Level Research Project [grant number 112004], National Natural Science Foundation of China [grant number 31860188] and the Applied Basic Research Programs of Yunnan Prov-

ince (2019FB067).

Conflicts of Interest

The authors declare no conflicts of interest regarding the publication of this paper.

References

[1] Santana, M.A.A., Dos Santos, F.S.N., Sousa, V.C., *et al.* (2008) Variability Sources of DC Voltage-Current Measurements in the Study of TiO_2-Based Varistors. *Measurement*, **41**, 1105-1112. https://doi.org/10.1016/j.measurement.2008.03.006

[2] Yan, M.F. and Rhodes, W.W. (1982) Preparation and Properties of TiO_2 Varistors. *Applied Physics Letters*, **40**, 536-537. https://doi.org/10.1063/1.93134

[3] Bueno, P.R., Varela, J.A. and Longo, E. (2008) SnO_2, ZnO and Related Polycrystalline Compound Semiconductors: An Overview and Review on the Voltage-Dependent Resistance (Non-Ohmic) Feature. *Journal of the European Ceramic Society*, **28**, 505-529. https://doi.org/10.1016/j.jeurceramsoc.2007.06.011

[4] Cassia-Santos, M.R., Sousa, V.C., Oliveira, M.M., Sensato, F.R., Bacelar, W.K., Gomes, J.W., Longo, E., Leite, E.R. and Varela, J.A. (2005) Recent Research Developments in SnO_2-Based Varistors. *Materials Chemistry and Physics*, **90**, 1-9. https://doi.org/10.1016/j.matchemphys.2003.12.014

[5] Metz, R., Koumeir, D., Morel, J., Pansiot, J., Houabes, M. and Hassanzadeh, M. (2008) Electrical Barriers Formation at the Grain Boundaries of Co-Doped SnO_2 Varistor Ceramics. *Journal of the European Ceramic Society*, **28**, 829-835. https://doi.org/10.1016/j.jeurceramsoc.2007.05.024

[6] Yang, S.L. and Wu, J.M. (1995) Effects of Nb_2O_5 in (Ba, Bi, Nb)-Added TiO_2 Ceramic Varistors. *Journal of Materials Research*, **10**, 345-352. https://doi.org/10.1557/JMR.1995.0345

[7] Meng, F.M., Lu, F., Xiao, L. and Sun, Z.Q. (2009) Influence of Soaking Time on Nonlinear Electrical Behavior and Dielectric Properties of TiO_2-Based Varistor Ceramics. *Journal of Central South University of Technology*, **16**, 897-901. https://doi.org/10.1007/s11771-009-0149-5

[8] Wang, W.Y., Zhang, D.F., Xu, T., Li, X.F., Zhou, T. and Chen, X.L. (2002) Effect of Temperature on Nonlinear Electrical Behavior and Dielectric Properties of (Ca, Ta)-Doped TiO_2 Ceramics. *Materials Research Bulletin*, **37**, 1197-1206. https://doi.org/10.1016/S0025-5408(02)00731-6

[9] Navale, S.C., Murugan, A.V. and Ravi, V. (2007) Varistors Based on Ta-Doped TiO_2. *Ceramics International*, **33**, 301-303. https://doi.org/10.1016/j.ceramint.2005.07.026

[10] Luo, S.H., Tang, Z.L., Li, J.Y. and Zhang, Z.T. (2008) Effect of Ta_2O_5 in (Ca, Si, Ta)-Doped TiO_2 Ceramic Varistors. *Ceramics International*, **34**, 1345-1347. https://doi.org/10.1016/j.ceramint.2007.03.005

[11] Zhao, J.Z., Wang, B.X. and Lu, K. (2014) Influence of Ta_2O_5 Doping and Microwave Sintering on TiO_2-Based Varistor Properties. *Ceramics International*, **40**, 14229-14234. https://doi.org/10.1016/j.ceramint.2014.06.012

[12] Gong, Y.Y., Chu, R.Q., Xu, Z.J., Sun, J., Chao, F.X., Ma, S., Hao, J., Li, H.Y. and Li, G.R. (2015) Electrical Properties of Ta_2O_5-Doped TiO_2 Varistor Ceramics Sintered at Low-Temperature. *Ceramics International*, **41**, 9183-9187.

https://doi.org/10.1016/j.ceramint.2015.03.082

[13] Gaikwad, A.B., Navale, S.C. and Ravia, V. (2005) TiO_2 Ceramic Varistor Modified with Tantalum and Barium. *Materials Science and Engineering*: *B*, **123**, 50-52. https://doi.org/10.1016/j.mseb.2005.06.015

[14] Luo, S.H., Yao, W.W., Li, H.Y., Zhang, Z.T. and Xiong, X.Z. (2005) The Role of Niobium in (Ca, Si, Ce, Nb)-Doped TiO_2 Varistors. *Key Engineering Materials*, **280**-**283**, 297-300. https://doi.org/10.4028/www.scientific.net/KEM.280-283.297

[15] Wang, W.Y., Zhang, D.F., Xu, T., Li, X.F., Zhou, T. and Chen, X.L. (2002) Nonlinear Electrical Behavior and Dielectric Properties of (Ca, Ta)-Doped TiO_2 Ceramics. *Journal of Alloys and Compounds*, **335**, 210-215. https://doi.org/10.1016/S0925-8388(01)01827-8

[16] Ekaphan, S., Krissana, P. and Thanin, P. (2019) A Novel Strategy to Improve the Thermal Stability of Dielectric Properties and Reduce the Dielectric Loss Tangent of $Ca_{1-1.5x}Pr_xCu_3Ti_4O_{12}/TiO_2$ Ceramics. *Ceramics International*, **45**, 14733-14741. https://doi.org/10.1016/j.ceramint.2019.04.199

[17] Yang, S.J., Zhu, D.C. and Peng, F.C. (2019) Effect of Doped Sb_2O_3 on the Electrical Properties of TiO_2-Based Cramics with the Dual Function of a Varistor-Capacitor. *Journal of Electronic Materials*, **48**, 898-903. https://doi.org/10.1007/s11664-018-6790-8

[18] Peng, F.C. and Zhu, D.C. (2018) Effect of Sintering Temperature and Ho_2O_3 on the Properties of TiO_2-Based Varistors. *Ceramics International*, **44**, 21034-21039. https://doi.org/10.1016/j.ceramint.2018.08.139

[19] Kang, K.Y., Xu, K.M., Zhu G., *et al*. (2018) Varistor Properties of TiO_2-Ta_2O_5-$CaCO_3$ Ceramics Doped with GeO_2. *Journal of the Ceramic Society of Japan*, **126**, 360-366. https://doi.org/10.2109/jcersj2.17145

[20] Mannam, R., Kumar, E.S., Nandita, D.G. and Ramachandra, R.M.S. (2017) Reversible *p*-Type Conductivity in H Passivated Nitrogen and Phosphorous Codoped ZnO Thin Films Using Rapid Thermal Annealing. *Applied Surface Science*, **400**, 312-317. https://doi.org/10.1016/j.apsusc.2016.12.146

[21] Priyadarshini, D.M., Ramanjaneyulu, M., Ramachandra, M.S.R. and Nandita, D.G. (2017) Effect of Annealing Ambient on SnO_2 Thin Film Transistors. *Applied Surface Science*, **418**, 414-417. https://doi.org/10.1016/j.apsusc.2016.11.233

[22] Zheng, M.J., Zhang, G.Z., Wang, X., Wan, J.X., Wu, H. and Liu, C. (2017) Effects of Post-Deposition Annealing on ZrO_2/n-GaN MOS Capacitors with H_2O and O_3 as the Oxidizers. *Nanoscale Research Letters*, **12**, Article No. 267. https://doi.org/10.1186/s11671-017-2024-x

[23] Hosokawa, A., Takagi, K. and Kuriiwa, T. (2017) Nanocomposite Nd-Fe-Ti-B Magnets Produced by Melt Spinning and Flash Annealing. *Journal of Magnetism and Magnetic Materials*, **439**, 220-227. https://doi.org/10.1016/j.jmmm.2017.05.023

[24] Zhao, J.Z., Zhang, C.G., Hu, C.Y. and Lu, K. (2017) Effect of Thermal Treatmenton TiO_2 Varistor Properties in Different Atmospheres. *Journal of the European Ceramic Society*, **37**, 3353-3359. https://doi.org/10.1016/j.jeurceramsoc.2017.04.021

[25] Liu, L., Fang, L., Huang,Y. , Li,Y., Shi, D., Zheng, S., Wu, S. and Hu, C. (2011) Dielectric and Nonlinear Current-Voltage Characteristics of Rare-Earth Doped $CaCu_3Ti_4O_{12}$ Ceramics. *Journal of Applied Physics*, **110**, 94-101. https://doi.org/10.1063/1.3658258

[26] Desousa, V.C., Oliveira, M.M., Orlandi, M., Leite, E.R. and Longo, E. (2006) (Ta, Cr)-Doped {T}{i}O_2 Electroceramic Systems. *Journal of Materials Science*: *Materials in Electronics*, **17**, 79-84. https://doi.org/10.1007/s10854-005-5145-4

[27] Xue, H., Guan, X.F. and Yu, R. (2009) Dielectric Properties and Current-Voltage Nonlinear Behavior of $Ca_{1-x}Sr_x$-$Cu_3Ti_4O_{12}$ Ceramics. *Journal of Alloys and Compounds*, **482**, L14-L17. https://doi.org/10.1016/j.jallcom.2009.03.190